Life Sciences 379 (2025) 123889

Contents lists available at ScienceDirect

Life Sciences

journal homepage: www.elsevier.com/locate/lifescie

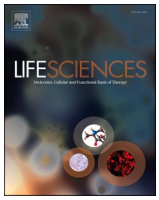

Notch activation downregulates EZH2 to thereby attenuate endothelial cell proliferation and angiogenesis via MYC destabilization

Yanyan Duan [a,b,1], Ting Wen [a,b,1], Jingli Ma [a], Yuxin Chen [a], Liang Liang [b], Ziyan Yang [b], Peiran Zhang [b], Quan Zhang [b,c], Manhong Li [c], Xingxing Feng [b], Danni Jia [b], Shanqiang Luo [b], Jiaxing Sun [c,*], Hua Han [b,d,*], Xianchun Yan [b,*]

[a] Institute of Future Agriculture, Northwest Agriculture and Forestry University, Yangling 712100, China
[b] State Key Laboratory of Holistic Integrative Management of Gastrointestinal Cancers, Department of Biochemistry and Molecular Biology, Fourth Military Medical University, Xi'an 710032, China
[c] Department of Ophthalmology, Xijing Hospital, Fourth Military Medical University, Xi'an 710032, China
[d] Tangdu Innovative Institute of Science and Technology, Tangdu Hospital, Fourth Military Medical University, Xi'an 710038, China

ARTICLE INFO

Keywords:
Notch
EZH2
MYC
Endothelial cell
Angiogenesis

ABSTRACT

Aims: Angiogenesis, a tightly regulated process involving dynamic endothelial cell (EC) proliferation, is critical in both physiological and pathological contexts such as ocular neovascular disorders. While Notch signaling is known to regulate angiogenesis, its downstream molecular mechanisms remain incompletely understood.
Main methods: Gene-modified mice with a Cdh5-Cre^{ERT} transgene were generated to block Notch signaling in ECs. Primary HUVECs were cultured in vitro. Gene expression were analyzed via qRT-PCR, western blotting, and immunofluorescence. Transcriptional regulation was investigated using reporter and ChIP assays. EC proliferation and migration were assessed through EdU incorporation, Transwell, and wound healing assays, respectively. Angiogenesis was evaluated in vivo using Matrigel plug, retinal angiogenesis, oxygen-induced retinopathy (OIR), and choroidal neovascularization (CNV) models.
Key finding: Notch activation upregulated, whereas Notch blockade downregulated EZH2 expression in both mRNA and protein levels. Mechanistically, Notch signaling directly suppresses EZH2 promoter activity, thereby transcriptionally repressing EZH2 expression. Functionally, EZH2 inhibition impaired EC proliferation and sprouting angiogenesis, while EZH2 overexpression enhanced these processes. Furthermore, EZH2 inhibition reversed the pro-angiogenic effects of Notch blockade. At the molecular level, EZH2 stabilized MYC protein by modulating Thr58 phosphorylation and regulating MYC stability factors, thereby preventing its proteasomal degradation. MYC overexpression rescued the angiogenesis defects caused by EZH2 inhibition. Importantly, EZH2 was upregulated in OIR and CNV models, and pharmacological EZH2 inhibition (GSK126) effectively suppressed pathological angiogenesis.
Significance: Our findings not only elucidate the novel role of EZH2 in mediating Notch function in angiogenesis but also provide a promising therapeutic strategy for treating neovascularization-related diseases with EZH2 inhibitors.

1. Introduction

Under the stimulation of various growth factors, particularly the vascular endothelial growth factor (VEGF), endothelial cells (ECs) undergo proliferation, tip/stalk differentiation, migration, and arterial-venous specification, and form new vascular networks to meet the increased demand of tissue perfusion [1,2]. This angiogenic process plays a pivotal role in both physiological tissue development and homeostasis, and pathological neovascularization in microvascular-related diseases as well [3]. In clinical practice, anti-angiogenic therapies (AATs), especially those employing VEGF-VEGF receptor (VEGFR) signal blockers, have shown significant efficacy in treating neovascular

* Corresponding authors.
E-mail addresses: sjxsjx001@163.com (J. Sun), huahan@fmmu.edu.cn (H. Han), yanxianchun@fmmu.edu.cn (X. Yan).
[1] These authors contributed equally to this study.

https://doi.org/10.1016/j.lfs.2025.123889
Received 16 May 2025; Received in revised form 15 July 2025; Accepted 25 July 2025
Available online 5 August 2025

disorders such as age-related macular degeneration (AMD) and retinopathy of prematurity (ROP) [1,4]. These therapeutic strategies primarily work by suppressing EC proliferation and modulating other relevant cellular processes, thereby effectively slowing disease progression [5]. Consequently, elucidating the fundamental mechanisms that regulate EC proliferation holds significant theoretical importance and translational potential for clinical applications.

The Notch signaling pathway serves as a critical regulator of EC proliferation, tip/stalk differentiation, and arterialization during angiogenesis [6–9]. Both published studies and our previous work have established that Notch activation downregulates the MYC proto-oncogene to thereby inhibit EC proliferation while promote arterial specification [7,10,11]. Moreover, Fernández-Chacón et al. recently demonstrated disruption of Notch signaling through Dll4 deletion potently activates MYC-dependent EC proliferation and promotes tip cell specification [12]. Mechanistically, Notch activation may repress MYC through different growth-related signaling pathways such as the PI3K-Akt signaling and Ras signaling [13]. We have recently been focusing on a panel of Notch downstream miRNAs, and have identified miR-218 and miR-342-5p could mediate the repression of MYC by Notch activation and consequently attenuate angiogenesis [10,11,14]. Nevertheless, whether Notch activation represses MYC via other downstream regulators in controlling EC functions and angiogenesis remains to be identified.

Enhancer of zeste homolog 2 (EZH2) is a catalytic subunit of the polycomb repressive complex 2 (PRC2), and responsible for mediating trimethylation of histone H3 at lysine 27 (H3K27me3), a modification associated with gene silencing. Beyond its well-established repressive function, emerging evidence suggests that EZH2 can also act as a transcriptional activator by methylating non-histone proteins or directly interacting with other regulatory factors, thereby promoting downstream gene expression independently of PRC2 [15]. In ECs, EZH2, modulated by shear stress and VEGFR signaling [16,17], has been shown to regulate EC proliferation, inflammation, and survival through multiple downstream molecules and signaling pathways, including PI3K/Akt, VEGFR2/ERK, eNOS, NF-κB, and non-coding RNAs [15,18]. EZH2 inhibition attenuates EC proliferation and angiogenesis under both physiological and pathological conditions [19,20]. Furthermore, emerging evidence suggested that EZH2 may interact with Notch or MYC to modulate proliferation and differentiation of other cells [21–24]. However, the precise upstream and downstream mechanisms of EZH2 and its therapeutic implications in angiogenesis and related diseases such as ocular neovascular diseases remain to be fully elucidated.

In this study, we demonstrated that Notch signaling transcriptionally represses EZH2 expression, consequently inhibiting EC proliferation and sprouting angiogenesis. Mechanistically, EZH2 downregulation destabilizes MYC protein, which in turn reduces the expression of key cell cycle regulators, ultimately impairing EC proliferation and angiogenesis. Notably, we identified substantial upregulation of EZH2 in pathological ECs associated with ocular neovascular disorders including choroidal neovascularization (CNV) and oxygen-induced retinopathy (OIR). Pharmacological targeting EZH2 effectively suppresses aberrant angiogenesis in both CNV and OIR animal models, highlighting its potential as a therapeutic strategy for these intraocular neovascular disorders.

2. Materials and methods

2.1. Animal models

C57BL/6 mice were maintained under specific pathogen-free (SPF) conditions. Cdh5-Cre^{ERT}, and *RBPJ*^{floxed} mice were described previously [25–27]. Polymerase chain reaction (PCR) was used for genotyping of mice and primers were listed in Supplementary Table S1. For induction of Cre-mediated recombination, male or female mice aged 6–8 weeks were intraperitoneally (i.p) injected daily with 100 μl tamoxifen (20 mg/ml, Sigma-Aldrich, St.Louis, MO, USA) for 5 days, while neonatal pups were subcutaneously (s.c) injected with 2.5 μl tamoxifen for 3 consecutive days from postnatal day 1 (P1). In some cases, pups were subcutaneously (s.c) injected daily with GSK126 (100 mg/kg, TargetMoI, Shanghai, China) or dimethyl sulfoxide (DMSO) from P3 to P6. Retinas were then harvested and fixed for subsequent immunostaining.

For the OIR model, pups and their mothers were placed in a high oxygen-chamber (75 ± 2 %) from P7 to P12 and then returned to conventional conditions as described before [28]. GSK126 (100 mg/kg), 10058-F4 (30 mg/kg) or DMSO were i.p injected every other day from P12. Retinas were collected and fixed for subsequent immunostaining on P17.

For the CNV model, mice were anesthetized, and their pupils were dilated with tropicamide. Five laser spots were then made between the major retinal vessels on both eyes of mice using a 532 nm laser beam (Iris Radiation Systems, USA; spot size 75 μm, power 100 mW, duration 0.1 s) as described before [28]. The disruption of Brush's membrane was further confirmed by the appearance of a cavitation bubble without any accompanying hemorrhage. GSK126 (100 mg/kg) or DMSO were i.p injected every other day from day 1 after photocoagulation and retinas were collected for subsequent staining on day 7.

For the Matrigel plug assay, 300 μl of Matrigel (BD Bioscience, San Jose, CA) containing 400 ng/ml VEGF and 250 ng/ml basic fibroblast growth factor (bFGF) (Sino Biological, Beijing, China) was imbedded along the dorsal midline on each side of mice. Mice were maintained for 7 days and Matrigel plugs were harvested for subsequent Masson's trichorme staining with a kit (Servicebio, Wuhan, China, G1006). All animal experiments were reviewed and approved by the Animal Experiment Administration Committee of the Fourth Military Medical University.

2.2. Histology

To analyze retinal and choroidal angiogenesis, retinas or the retinal-pigment epithelium (RPE)-choroid-sclera complex tissues were fixed in 4 % paraformaldehyde (PFA), blocked and permeabilized in PBS containing 1 % bovine serum albumin (BSA) and 0.5 % Triton X-100 overnight at 4 °C. Tissues were then immunostained with anti-CD31 antibody (Biolegend, San Diego, CA), followed by incubating with Alexa Fluor 594-conjugated donkey anti-rat IgG secondary antibody (Invitrogen, Carlsbad, CA). Samples were then flat-mounted, and photos were captured under a confocal laser scanning microscope (A1R, Nikon, Tokyo, Japan). To quantify the vascular density, capillary loops or neovascular areas were determined and compared between different groups by Image-Pro Plus 6.0 software as previous described [28].

For immunofluorescence, tissues were fixed in 4 % PFA at 4 °C for 4 h, followed by dehydration in 30 % sucrose in PBS overnight. Samples were embedded in optimal cutting temperature (OCT) compound (Sakura Finetek, Inc., Torrance, CA), cryosectioned at 8 μm thickness, and dried for 2 h at room temperature. Sections were then blocked with 1 % BSA in PBS, permeabilized with 0.5 % Triton X-100, and incubated overnight at 4 °C with primary antibodies. After washing, sections were incubated with secondary antibodies at room temperature for 1 h. Images were captured under a fluorescence or laser-scanning confocal fluorescence microscopes (A1R). Cell samples were fixed with 4 % PFA for 30 min at room temperature, permeabilized with 0.3 % Triton X-100, and blocked in 5 % BSA for 30 min at room temperature. Samples were stained in the same way and nuclei were counter-stained with Hoechst 33258 (Sigma-Aldrich).

2.3. Cell culture and transfection

Primary human umbilical vein endothelial cells (HUVECs) were isolated from human umbilical cord biopsies obtained from the Department of Gynecology and Obstetrics in Xijing hospital, and

cultured in complete endothelial cell medium (ECM, ScienCell, San Diego, CA) as previously described [25]. HUVECs of passages 3 to 6 were used for subsequent experiments. The use of human samples was approved by the Ethics Committee of Xijing Hospital, Fourth Military Medical University.

To induce Notch activation in vitro, HUVECs were infected with adenovirus expressing human Notch1 intracellular domain (NICD) (AdNIC, HanBiol, Shanghai, China) at a multiplicity of infection (MOI) of 50 or treated with soluble Delta-like 4 (Dll4) proteins (Sino Biological Inc., Beijing, China) coated on culture dishes at the concentration of 1 μg/ml as previously described [10,11]. To block Notch signal, HUVECs were treated with the γ-secretase inhibitor DAPT (Selleck Chemicals, Houston, TX) at the concentration of 25 μmol/l. To induce EZH2 blockade, GSK126 or DNZep were purchased from TargetMoI and used at the concentration of 10 μmol/l. To knock down the EZH2 level in vitro, HUVECs were transfected with EZH2 siRNA (Genepharma, Shanghai, China) at the concentration of 50 nmol/l. To overexpress EZH2 or MYC, HUVECs were infected with adenovirus expressing MYC or EZH2 or control virus (HanBio) at an MOI of 100, as previously mentioned [10,11]. For MYC inhibition, HUVECs were treated with 10058-F4 (TargetMoI) at the concentration of 10 μmol/l. For the protein decay assay, HUVECs were treated with MG-132 or cycloheximide (CHX, Selleck Chemicals) at the concentration of 50 mmol/l or 50 mg/ml, respectively.

2.4. Cell proliferation and migration

To evaluate cell proliferation, HUVECs were incubated with medium containing 50 μmol/l EdU (RiboBio, Guangzhou, China) for 2 h, fixed with 4 % PFA at room temperature for 30 min, followed by staining with Apollo 567 and Hoechst according to the manufacturer's instructions. Alternatively, HUVECs were fixed, permeabilized, blocked and incubated with anti-Ki67 antibody (Abcam), followed by incubating with Alexa Fluor 594-conjugated donkey anti-rabbit IgG secondary antibody (Invitrogen). Images were captured under a fluorescent microscope and the cell proliferation ability was determined by the percentage of EdU^+ or $Ki67^+$ cells.

To evaluate cell migration, the wound healing assay and Transwell assay were performed. For the wound healing assay, a scratch was created with a pipette tip, and the medium was then replaced by ECM supplemented with 0.5 % FBS. Wound closure was measured under a microscope. For the Transwell assay, HUVECs were harvested and seeded into the upper chamber of Transwell unit (Corning) at a total number of 1×10^5 cells, and complete ECM was added to the lower chamber. Cells were cultured for 12 h and fixed by 4 % PFA, and stained with crystal violet. Number of cells migrating to the lower membrane was observed under a microscope.

2.5. Fibrin beads assay

A fibrin beads assay was performed using a fibrin beads assay kit (Amersham-Pharmacia Biotech) as previously described [25]. Briefly, HUVECs were incubated with Cytodex 3 microcarrier beads (400 cells per bead) at 37 °C for 4 h and then transferred into a 12-well plate and left overnight. The beads were embedded in fibrinogen (Sigma-Aldrich) containing 0.625 U/ml thrombin (Sigma-Aldrich) at a density of 100 beads/ml in a 48-well plate, and MRC5 cells (2×10^5 cells per well) in 0.5 ml EGM-2 medium were added. The medium was changed every other day. The average number of sprouts per bead and the average sprout length were calculated for each independent sample.

2.6. Quantitative reverse transcription-polymerase chain reaction (qRT-PCR)

Cells were lysed with the Trizol reagent (Sigma-Aldrich). RNA was extracted and reverse transcribed into complementary DNA (cDNA) using a reverse transcription kit (Takara Biotechnology, Dalian, China). Real-time PCR was performed using a SYBR Premix Ex Taq kit (Takara Biotechnology) and a Quant-Studio 5 real-time PCR system (Life Technologies, Waltham, MA, USA). Gene expression level was evaluated as relative fold-change with β-actin as an internal control. For data analysis, the control sample value from one group was first normalized to 1, all other samples in the same experimental run were then compared relative to this reference control. The primer sequences are listed in supplementary Table S1.

2.7. Western blotting

Cells were lysed with the radio-immunoprecipitation assay (RIPA) buffer (Beyotime, Shanghai, China) containing phenylmethylsulfonyl fluoride (PMSF, Sigma-Aldrich). Proteins were isolated and separated by sodium dodecyl sulfate-polyacrylamide gel electrophoresis (SDS-PAGE) and transferred onto polyvinylidene fluoride membranes. The membranes were then blocked and incubated with primary antibodies at 4 °C overnight, followed by the corresponding horse-radish peroxidase (HRP) – conjugated secondary antibodies. Primary antibodies included anti-EZH2 (1:1000, Abcam), anti-MYC (1:1000, CST, Boston, MA, USA), anti-H3K27me3 (1:1000, CST), anti-phosphorylated MYC (pT58) (1:1000, Biodragon, Suzhou, Jiangsu, China), anti-AURKB (1:1000, Biodragon), anti-β-ACTIN (1:5000, Proteintech, Chicago, IL, USA). Bands were developed using an enhanced chemiluminescence (ECL) system (Clinx Science Instruments, Shanghai, China). Images were analyzed using the ImageJ2x software (Rawak Software, Stuttgart, Germany). For data analysis, the control sample value from one group was first normalized to 1, all other samples in the same experimental run were then compared relative to this reference control.

2.8. Reporter assay

The EZH2 promoter fragment (−1238 bp ~ +100 bp) was synthesized and cloned into the pGL3-basic plasmid (Promega, WI, USA) to construct the pGL3-EZH2-pro plasmid. HEK293T cells were infected with adenovirus expressing NICD (AdNIC) or control, together with pGL3-EZH2-pro (100 ng) or pGL3-basic (100 ng) and phRL-TK (5 ng) for 48 h. Cells were lysed, and the firefly and renilla luciferase activities were analyzed using a dual luciferase reporter assay system (Promega).

2.9. Chromatin immunoprecipitation (ChIP) assay

ChIP assay was performed using a commercial kit (CST) according to the supplier's instructions. Briefly, HUVECs were fixed with 1 % formaldehyde and quenched with 1.25 mol/l glycine. Cells were then washed and lysed in 0.5 % SDS lysis buffer at 4 °C for 30 min. Supernatants were incubated with anti-HES1 antibody (CST) at 4 °C for 12 h. Protein A/G beads were then added and incubated at room temperature for 2 h. The precipitates were then reverse crosslinked, and DNA was purified and the target fragments were quantified by qPCR. Relative enrichment was determined as the percentage of input (%) = 2 % x 2 (Ct of input – Ct of sample) and compared with the IgG group. The primer sequences are listed in supplementary Table S1.

2.10. Statistical analysis

Statistical analysis was conducted using Image-Pro Plus6.0, GraphPad Prism 8.0 and GSEA2–2.2.3 software. All quantitative data were presented as means ± standard deviation (SD). Statistical significance was calculated using Student's *t*-tests or one-way ANOVA followed by Tukey's post hoc test. Nonparametric tests were used for non-normally distributed data. $p < 0.05$ was considered statistically significant.

3. Results

3.1. EZH2 is downregulated by Notch activation in ECs

The Notch signaling pathway plays a crucial role in regulating EC proliferation, tip/stalk specification, arterial-venous specification during angiogenesis, at least partly via repressing MYC [7,10–12,29]. To further identify molecules mediating the effect of Notch activation, we first analyzed a public transcriptome dataset of ECs isolated on different days during retinal vascular development (GSE8678). The results revealed a gradual decrease in EZH2 expression as EC transitioned from a proliferating to a quiescent state, and an inverse correlation with the expression of Notch signaling-related genes (Fig. 1A). Analysis of another published transcriptomic data from Notch-activated versus control ECs (GSE45750) demonstrated significantly reduced expression of EZH2 downstream target genes in Notch-activated group (Fig. 1B). Subsequent in vitro experiments using adenovirus-mediated NICD overexpression (AdNIC) showed that both mRNA and protein levels of EZH2 were markedly decreased in Notch-activated ECs, as confirmed by qRT-PCR and Western blotting (Fig. 1C and D). Notably, this suppressive effect exhibited sustained persistence (Fig. S1A). Conversely, pharmacological inhibition of Notch signaling using DAPT resulted in upregulation of EZH2 at both mRNA and protein levels (Fig. 1E and F). To evaluate whether Notch activation downregulates EZH2 by repressing the EZH2 promoter, which harbors putative binding sites for Notch downstream repressors HES1 and HEY1 [30], we constructed a reporter and performed the reporter assay (Fig. 1G). The result showed that Notch activation by NICD overexpression significantly repressed the EZH2 promoter (Fig. 1H). Further ChIP experiments revealed that the Notch downstream effector HES1 could efficiently bind to the 3 potential sites in the EZH2 promoter (Fig. 1I) [31]. Taken together, these results suggest that Notch activation transcriptionally represses EZH2 expression in ECs.

3.2. EZH2 is required for EC proliferation and angiogenesis

To investigate the role of EZH2 in ECs, we performed a reanalysis of published RNA sequencing (RNA-seq) data (GSE71164), and the result revealed that EZH2 knockdown significantly downregulated genes associated with cell cycle and proliferation (Fig. S2 A-E). To further validate these findings, we employed siRNA-mediated silencing and pharmacological inhibition of EZH2 using GSK126 or DNZep. Consistently, EdU incorporation assay and Ki67 immunofluorescence staining confirmed that EZH2 inhibition markedly suppressed EC proliferation (Fig. 2A and B; S3A-C). Meanwhile, qRT-PCR revealed concomitant downregulation of multiple proliferation-related genes following EZH2 inhibition (Fig. S3D). In contrast, Transwell and wound healing assays showed that EZH2 inhibition did not significantly affect EC migration (Fig. S3E and F). To assess the functional consequences of EZH2 modulation on angiogenesis, we performed a fibrin bead assay, and the result

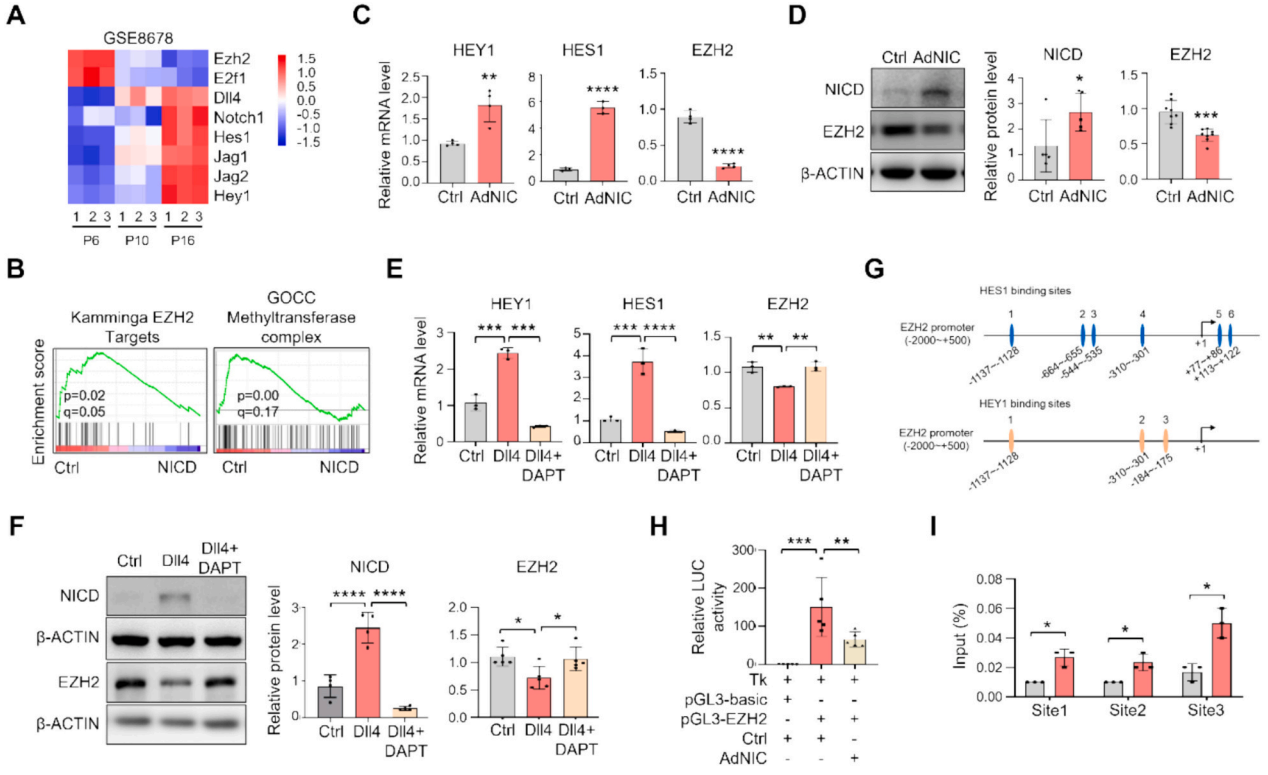

Fig. 1. Notch signal downregulates EZH2 expression in ECs. A Heatmap depicting differential expression pattern of EZH2 and Notch signaling-related genes in retinal ECs isolated from postnatal mice at indicated developmental time points (GSE8678 dataset). B GSEA demonstrating significant enrichment of EZH2 target genes and methyltransferase complex-associated genes in Ctrl versus NICD overexpressing groups (GSE45750). C qRT-PCR analysis of HEY1, HES1 (Notch signal markers) and EZH2 mRNA levels in HUVECs following 48 h infection with NICD-overexpressing (AdNIC) or control adenovirus ($n = 3$). D Western blotting analysis of NICD ($n = 5$) and EZH2 ($n = 8$) protein expression in HUVECs treated as in (C). E qRT-PCR quantification of HEY1, HES1 and EZH2 mRNA level in HUVECs cultured for 48 h on DLL4-coated or control dishes with/without DAPT inhibitor ($n = 3$). F Western blot analysis of NICD and EZH2 protein expression in HUVECs treated as in (E) ($n = 4$ for NICD, n = 5 for EZH2). G Schematic representation of the HES1 and HEY1 binding sites within the EZH2 promoter region, as identified using the JASPAR online prediction tool. H Dual-luciferase reporter assay evaluating EZH2 promoter activity in HEK293T cells co-transfected with pGL3-EZH2-pro/pGL3-control plus phRL-TK, followed by NICD-overexpressing or control adenovirus infection (n = 5). I ChIP analysis of HES1 binding to the EZH2 promoter in HUVECs. Cells were immunoprecipitated with either anti-HES1 antibody or control IgG, followed by qRT-PCR analysis of the enriched EZH2 promoter fragments ($n = 3$). Bars = means ± SD. *, $p < 0.05$; **, $p < 0.01$; ***, $p < 0.001$; ****, $p < 0.0001$. Statistical tests: two-tailed Student's *t*-test for C – D, I; one-way ANOVA followed by Tukey's post hoc test for E – F, H.

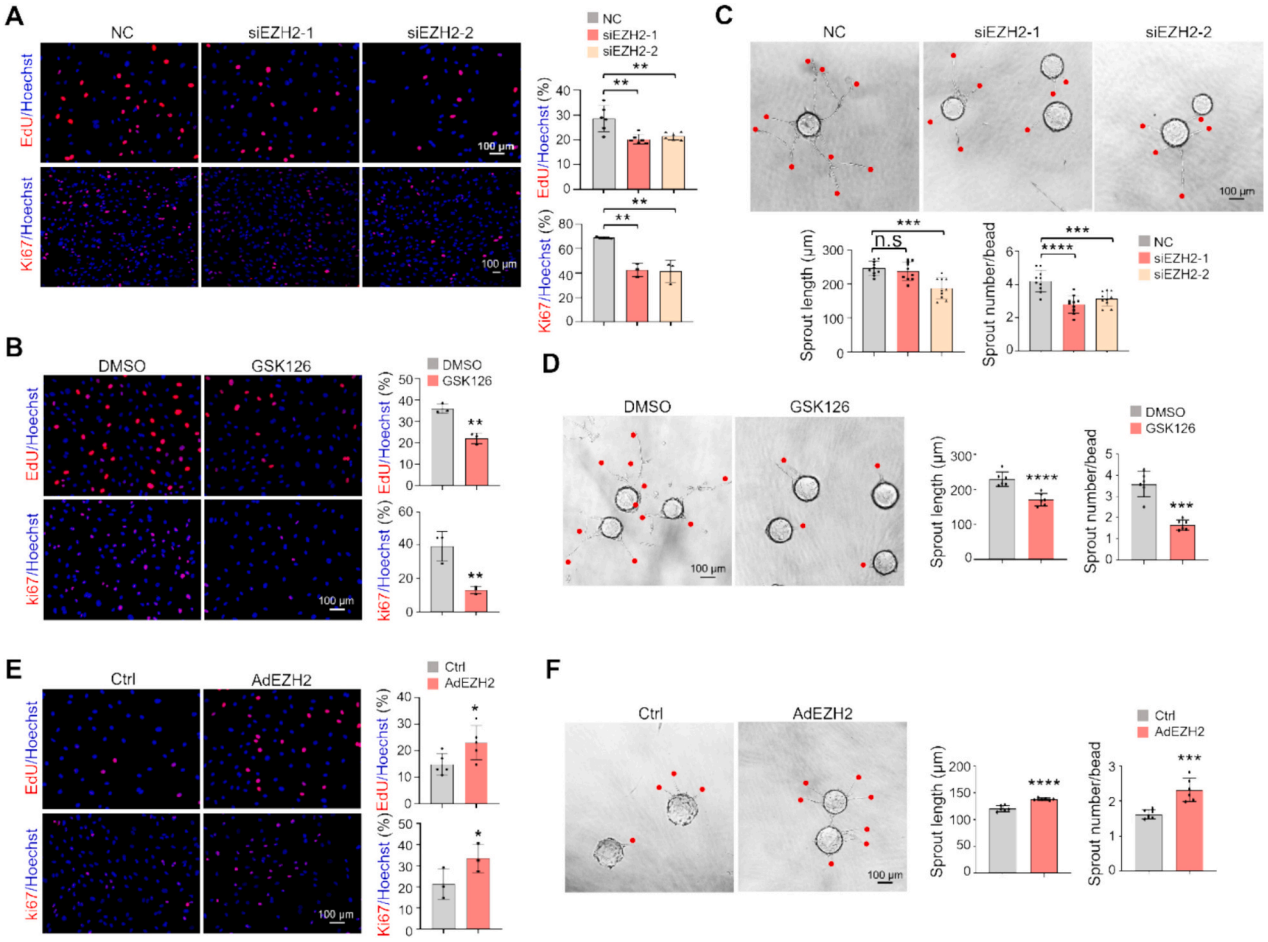

Fig. 2. EZH2 modulates EC proliferation and angiogenic sprouting in vitro. A HUVECs were transfected with EZH2-targeting siRNA for 48 h. EC proliferation was assessed using EdU incorporation assay ($n = 6$) and Ki67 immunofluorescence ($n = 3$). B HUVECs were treated with EZH2 inhibitor GSK126 for 48 h. EC proliferation was evaluated by EdU assay (n = 3) and Ki67 immunofluorescence (n = 3). C siRNA-mediated EZH2 knockdown in HUVECs followed by fibrin bead-based angiogenesis assay for 4 days. Sprout length and number were quantified ($n = 10$). D HUVECs were treated with GSK126 during fibrin bead assay for 4 days. Sprout length and number were analyzed ($n = 6$). E Adenovirus overexpression of EZH2 (AdEZH2) in HUVECs for 48 h. EC proliferation was determined by EdU assay (n = 5) and Ki67 immunofluorescence (n = 3). F EZH2-overexpressing HUVECs in fibrin bead assay with quantification of sprout length and number (n = 6). Bars = means ± SD. *, $p < 0.05$; **, $p < 0.01$; ***, $p < 0.001$; n.s, not significant. Statistical tests: two-tailed Student's *t*-test for B, D, E - F; one-way ANOVA followed by Tukey's post hoc test for A and C.

showed that EZH2 blockade significantly impaired EC sprouting (Fig. 2C and D). Conversely, adenovirus-mediated EZH2 overexpression enhanced both proliferation and sprouting of HUVECs (Fig. 2E and F; S3G and H). Collectively, these findings demonstrate that EZH2 is required for EC proliferation and sprouting angiogenesis.

Extensive evidence has established Notch signaling as a master regulator of endothelial tip/stalk cell fate and arterial-venous specification during angiogenesis [7,8,11,12]. To assess the potential role of EZH2 in regulating tip/stalk cell differentiation and arterial specification, we examined EZH2-mediated control using multiple approaches. Analysis of RNA-seq data and qRT-PCR validation demonstrated that EZH2 knockdown did not significantly alter the expression of tip/stalk cell markers (Fig. S4A-C) [32]. Meanwhile, EZH2 overexpression failed to rescue the inhibitory effects of Notch activation on tip cell markers or counteract the Notch-mediated upregulation of stalk cell markers (Fig. S4D), suggesting functional independence in tip/stalk cell differentiation between Notch and EZH2. Furthermore, although EZH2 knockdown elicited modest upregulation of both the arterial marker EFNB2 and venous marker EPHB4, the overall arteriovenous markers remained largely unaffected (Fig. S4E-G). Additionally, EZH2 overexpression did not interfere with the ability of Notch activation to upregulate arterial markers (Fig. S4H). Together, these data indicate that EZH2 might not be a major modulator of tip/stalk cell differentiation or arterial specification, and is not involved in Notch-dependent control of these processes.

3.3. Notch activation attenuates EC proliferation and angiogenesis by downregulating EZH2

To further investigate the role of Notch signaling-mediated EZH2 suppression in EC proliferation and angiogenesis, we blocked Notch signaling and examined the effect of EZH2 inhibition on EC proliferation. EdU staining revealed that EZH2 inhibition with GSK126 attenuated the enhanced EC proliferation induced by Notch blockade (Fig. 3A). On the other hand, EZH2 overexpression rescued the impaired proliferative capacity caused by Notch activation (Fig. 3B). Furthermore, EZH2 inhibition suppressed the Notch blockade-induced increase in sprouting angiogenesis (Fig. 3C and D). To extend these findings in vivo, we generated EC-specific RBPj knockout mice in which the canonical Notch signaling is blocked in ECs, and angiogenesis was evaluated with the Matrigel plug assay and the retinal neovascularization. The results demonstrated that Notch blockade in ECs led to enhanced angiogenesis, which was significantly attenuated by GSK126-induced EZH2 blockade (Fig. 3E and F). Overall, these findings indicate that Notch activation suppresses EC proliferation and angiogenesis through downregulation of EZH2.

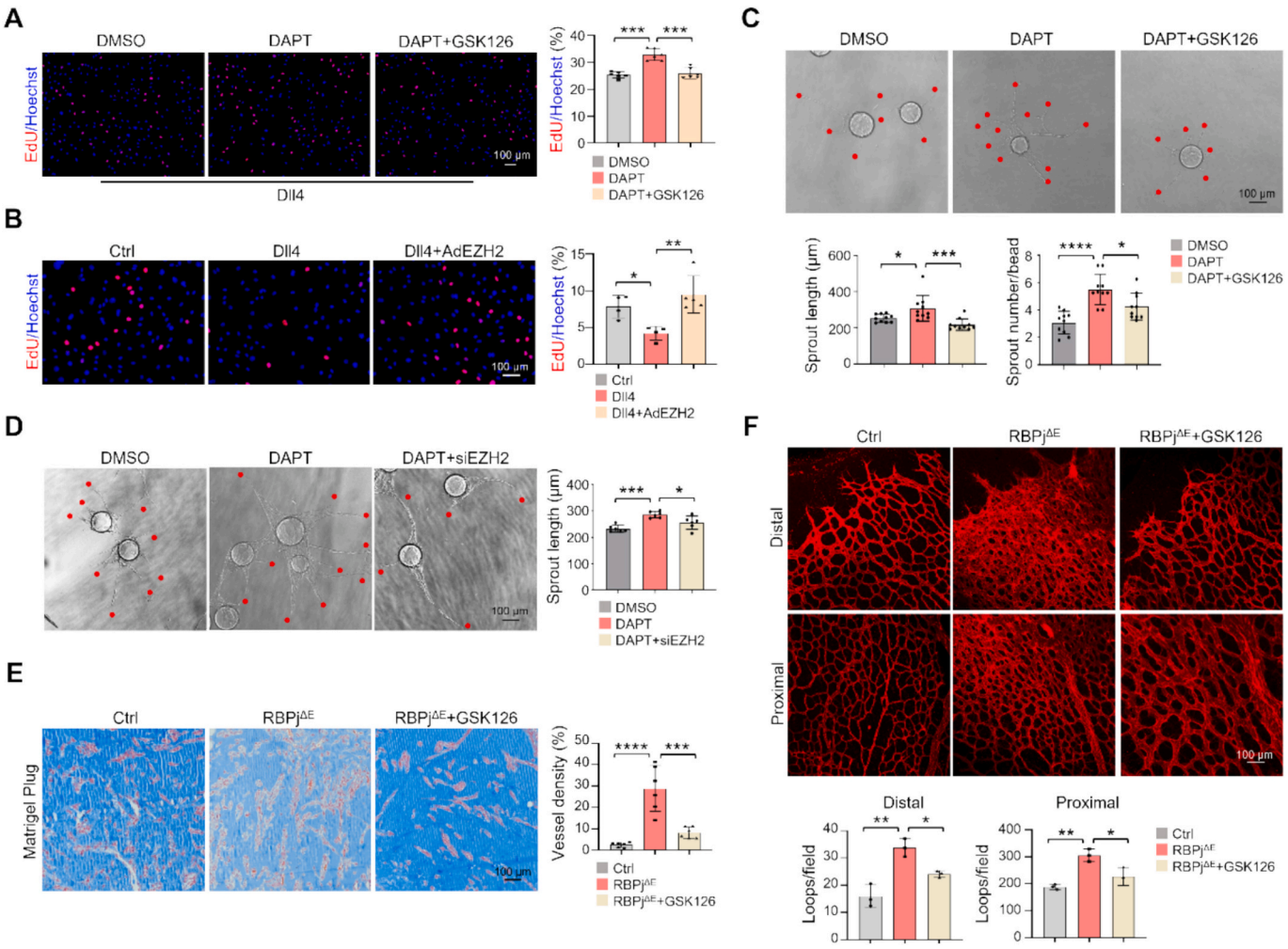

Fig. 3. EZH2 inhibition rescues hyper-angiogenesis caused by Notch signal blockade. A HUVECs were cultured on DLL4-coated dishes with/without DAPT or GSK126 for 48 h. EC proliferation was assessed by EdU assay (n = 6). B HUVECs infected with adenovirus overexpressing EZH2 or control were cultured on Dll4-coated or uncoated dishes for 48 h, followed by EdU assay to evaluate proliferation ($n = 4$). C Fibrin bead sprouting assay of HUVECs treated with DAPT alone or in combination with GSK126 for 4 days. Sprout length and number were quantified (n = 10). D Fibrin bead sprouting assay of HUVECs treated with DMSO or DAPT or DAPT in combination with EZH2-targeting siRNA for 4 days. Sprout length and number were quantified (n = 6). E Endothelial cell specific RBPj knockout ($RBPj^{\triangle E}$) or Ctrl mice were subcutaneously injected with Matrigel containing GSK126 or DMSO. After 7 days, plugs were harvested, sectioned, and stained with Masson's trichrome. Vessel density was quantified (n = 5). F $RBPj^{\triangle E}$ or Ctrl pups received daily subcutaneous injections of GSK126 or DMSO from P1 to P3. At P6, retinas were immunostained for CD31, and vascular loop density in distal/proximal regions was quantified ($n = 3$ mice per group). Bars = means ± SD. *, $p < 0.05$; **, $p < 0.01$; ***, $p < 0.001$; ****, $p < 0.0001$. Statistical tests: one-way ANOVA followed by Tukey's post hoc test for A - F.

3.4. EZH2 inhibition downregulates MYC expression by reducing its protein stability

To further elucidate the downstream regulatory mechanisms of EZH2, we performed analysis of the transcriptomes of EZH2 knockdown and control ECs. The results demonstrated significant downregulation of MYC downstream genes in EZH2 blockade group (Fig. 4A). Notably, MYC-regulated genes associated with cell proliferation, including those metabolic pathways involving glycolysis, tricarboxylic acid (TCA) cycle, and nucleotide metabolism, showed marked reduced expression upon EZH2 knockdown (Fig. S5A) [33,34]. qRT-PCR analysis revealed that key enzymes involved in nucleotide metabolism were substantially downregulated (Fig. S5B-D). Further experimental validation confirmed that EZH2 blockade led to a pronounced reduction in MYC protein expression, although it did not significantly affect MYC mRNA level (Fig. 4B-E). Furthermore, EZH2 overexpression could rescued the downregulation of MYC protein level induced by Notch activation (Fig. 4F). These results demonstrate that EZH2 does not regulate MYC gene expression in ECs, but significantly affects MYC protein levels.

Extensive studies have established that MYC protein levels are tightly regulated through post-translational mechanisms [33,34]. Prior studies have suggested that EZH2 could protect MYC protein stability [24]. To investigate this further, we assessed MYC protein turnover using MG132, a proteasome inhibitor. Our results demonstrated that blockade of proteasomal degradation completely rescued EZH2-mediated MYC downregulation (Fig. 4G; S6A). Moreover, CHX chase assays showed that EZH2 inhibition markedly enhanced MYC degradation (Fig. 4H). Consistent with these observations, EZH2 inhibition led to a pronounced increase in MYC phosphorylation at threonine 58 (T58) (Fig. 4I), a phosphorylation pattern recognized by E3 ligases such as FBW7, leading to MYC protein degradation [11,35,36]. Furthermore, EZH2 inhibition led to coordinated transcriptional reprogramming, characterized by downregulation of MYC-stabilizing factors and concurrent upregulation of MYC-destabilizing genes (Fig. S6B and C) [37–40]. Notably, we identified AURKB, a known direct regulator of MYC protein phosphorylation and stability [37], as being markedly downregulated at both mRNA and protein levels following EZH2 inhibition (Fig. 4I; S6B and C). In contrast, the expression levels of miR-218 and miR-342-5p, known

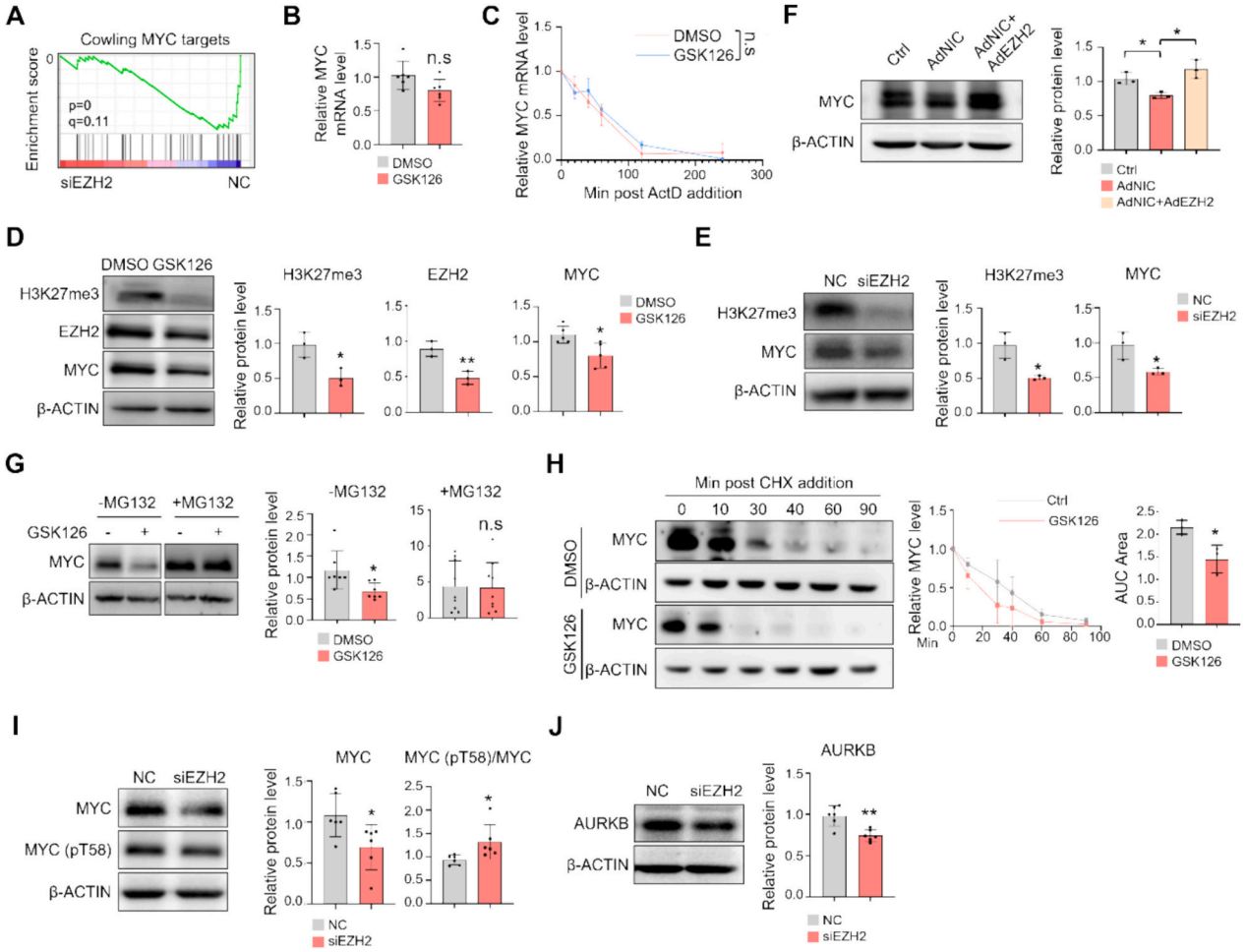

Fig. 4. EZH2 inhibition promotes MYC protein destabilization. A GSEA showing significant enrichment of MYC target genes in EZH2-knockdown (siEZH2) HUVECs compared with control cells from a published dataset (GSE71164). B qRT-PCR analysis of MYC mRNA expression in HUVECs treated with GSK126 or DMSO for 48 h (n = 6). C MYC mRNA stability assay: HUVECs treated as in (B) were exposed to ActD, with MYC transcript levels quantified by qRT-PCR at indicated time points (n = 3). D Western blotting analysis of H3K27me3, EZH2 and MYC protein levels in HUVECs treated as in (B) (n = 3 for H3K27me3 and EZH2; *n* = 4 for MYC). E Western blotting demonstrating reduced H3K27me3 and MYC protein expression following EZH2 siRNA-mediated knockdown compared with Ctrl. F Western blotting demonstrating MYC protein expression in HUVECs transfected with AdNIC, AdNIC+AdEZH2 or Ctrl (n = 3). G Proteasome inhibition assay: MYC protein levels were assessed by western blot in cells treated as in (B) with or without MG-132 (*n* = 7). H Protein stability analysis: CHX chase assay showing MYC degradation kinetics in GSK126- versus DMSO-treated HUVECs. Relative MYC protein levels compared with 0 min and area under curve (AUC) quantification are presented (n = 3). I Western blot analysis of MYC phosphorylation at threonine 58 (pT58) (n = 6) in EZH2 knockdown versus control cells. J Western blot analysis of AURKB protein level under EZH2 knockdown (n = 6). Bars = means ± SD. *, $p < 0.05$; **, $p < 0.01$; n.s, not significant. Statistical tests: two-tailed Student's *t*-test for B - E, G-J; one-way ANOVA followed by Tukey's post hoc test for F.

mediators of MYC stability downstream of Notch signaling, remained unaltered upon EZH2 depletion (Fig. S6D) [10,11]. These findings suggest a post-translational regulatory mechanism whereby EZH2 governs MYC protein abundance primarily by enhancing its stability.

3.5. EZH2 promotes EC proliferation and angiogenesis through MYC

To further elucidate the impact of EZH2 in regulating MYC-dependent EC proliferation and angiogenesis, we treated HUVECs with the EZH2 inhibitor while overexpressed MYC using virus-mediated transfection (Fig. 5A). EdU incorporation assay revealed that MYC overexpression effectively restored the diminished proliferation induced by EZH2 suppression (Fig. 5B), whereas pharmacological inhibition of MYC abolished the pro-proliferative effect of EZH2 overexpression (Fig. 5C). Additionally, MYC overexpression significantly rescued the angiogenesis defects induced by EZH2 suppression (Fig. 5D). Taken together, these results demonstrate that MYC is a critical downstream mediator of EZH2 in regulating EC proliferation and angiogenesis.

3.6. EZH2 inhibition compromises pathological ocular angiogenesis

Next, we evaluated the therapeutic potential of targeting EZH2 in pathological neovascularization. Initial analysis of published single-cell RNA sequencing (scRNA-seq) data (PRJNA864092) revealed significant upregulation of EZH2 and proliferation-associated genes in ECs from the OIR model [41], which was further validated by GSEA (Fig. 6A and B). To evaluate the translational potential, we employed two well-established murine models, OIR and laser-induced CNV, which mimic ROP and AMD, respectively [28]. Immunofluorescence staining confirmed robust EZH2 upregulation in ECs of pathological neovessels in both models (Fig. 6C and D). Pharmacological inhibition of EZH2 using GSK126 markedly attenuated intraocular pathological angiogenesis, as demonstrated by reduced $CD31^+$ vascular outgrowth in both models (Fig. 6E and F). Similarly, MYC inhibition with the 10058-F4 compound effectively suppressed pathological angiogenesis in the OIR model (Fig. S7). These findings collectively indicate that EZH2 represents a potential therapeutic target for ocular neovascularization-related disorders.

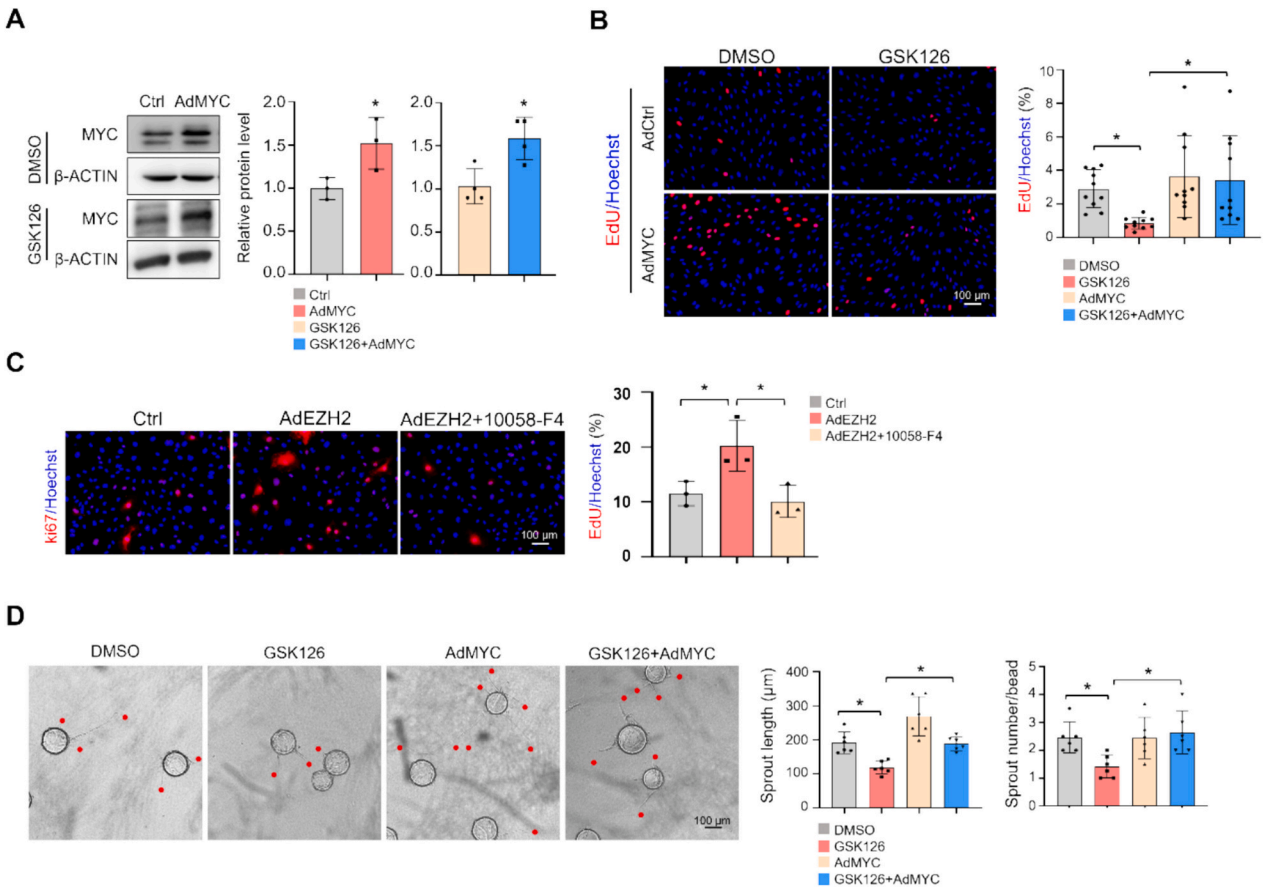

Fig. 5. MYC overexpression rescues EZH2 inhibition-induced impairment of EC proliferation and angiogenic capacity. A MYC expression in HUVECs was analyzed by Western blotting after 48 h of treatment with GSK126 or DMSO, together with AdMYC or Ctrl (n = 3 for DMSO, n = 4 for GSK126). B EdU incorporation assay showing proliferative capacity of HUVECs treated as in (A) (n = 10). C Adenovirus overexpression of EZH2 plus treatment of DMSO or 10058-F4 in HUVECs for 48 h. HUVEC proliferation was evaluated by Ki67 immunofluorescence. D Fibrin bead angiogenesis assay quantifying sprout length and number in HUVECs treated as in (A) (n = 6). Bars = means ± SD. *, $p < 0.05$. Statistical tests: two-tailed Student's *t*-test for A; one-way ANOVA followed by Tukey's post hoc test for B - D.

4. Discussion

Extensive research, including our previous studies, has established that Notch signaling attenuates MYC expression through diverse downstream mechanisms to modulates EC proliferation, tip/stalk cell specification, and arterial-venous specification, consequently inhibiting angiogenesis while preserving vascular homeostasis [7,10,11,13,14]. In the current study, we elucidated a novel mechanistic pathway wherein Notch signaling transcriptionally represses EZH2 expression. This suppression results in diminished MYC protein stability, ultimately impairing EC proliferation and angiogenesis (Fig. 7). Notch signaling pathway has been shown to transcriptionally repress downstream target genes through its effector transcription factors, HES1 and HEY1, which can regulate angiogenesis either independently or cooperatively [30,42–44]. Our results identified potential binding sites for both HES1 and HEY1 within the EZH2 promoter region. ChIP assays validated HES1 binding, but whether HEY1 similarly interacts with the EZH2 promoter remains to be determined. Moreover, further investigation is also needed to elucidate whether Notch-mediated transcriptional repression of EZH2 depends on HES1 or HEY1 individually or necessitates their synergistically activity [42].

Previous studies have documented the complex regulation of EZH2 expression in ECs, involving multiple signaling cascades (including HIF-1α and VEGF pathways), inflammatory mediators, hemodynamic forces, and epigenetic regulators [16,45–48]. Notably, our recent work has shown that EZH2 expression is negatively regulated by shear stress – a critical determinant of EC quiescence and survival [16,17]. Given that Notch functions as a mechanosensitive receptor capable of transducing hemodynamic signals [11,49], and intriguing unanswered question is whether Notch mediates the effects of shear stress on EZH2 regulation. Tsou et al. previously established that EZH2 can repress Notch signaling through transcriptional silencing of the Notch ligand DLL4 [50], the potential existence of a reciprocal negative feedback loop between Notch EZH2 warrants further investigation. Furthermore, the regulatory network between Notch signaling and EZH2 may exhibit higher-order complexity within the in vivo microenvironment [51]. This complexity stems from: spatiotemporal specificity during vascular development; dynamic crosstalk between Notch and other critical pathways (e.g., VEGF) [29]. To systematically decipher this regulatory network, future studies could integrate multi-omics profiling with high-resolution intravital imaging [52,53], thereby elucidating the dynamic regulatory mechanisms of the Notch-EZH2 axis during angiogenesis in vivo.

Sprouting angiogenesis, a complex morphogenetic process, critically depends on EC proliferation [54], where its targeted suppression alone is sufficient to impair angiogenic sprouting [55,56]. EZH2 was reported to be upregulated under hypoxia and pro-angiogenic factors such as VEGF, enhances EC proliferation, migration, and angiogenic potential [20,45,47], whereas its inhibition exerts opposing effects [16]. Our current findings suggested that genetic (siRNA) and pharmacological (small-molecule inhibitor) blockade of EZH2 significantly attenuated EC proliferation and sprouting angiogenesis but did not markedly affect migration, further supporting a pro-angiogenic role for EZH2 in these processes. However, the regulatory function of EZH2 in EC proliferation,

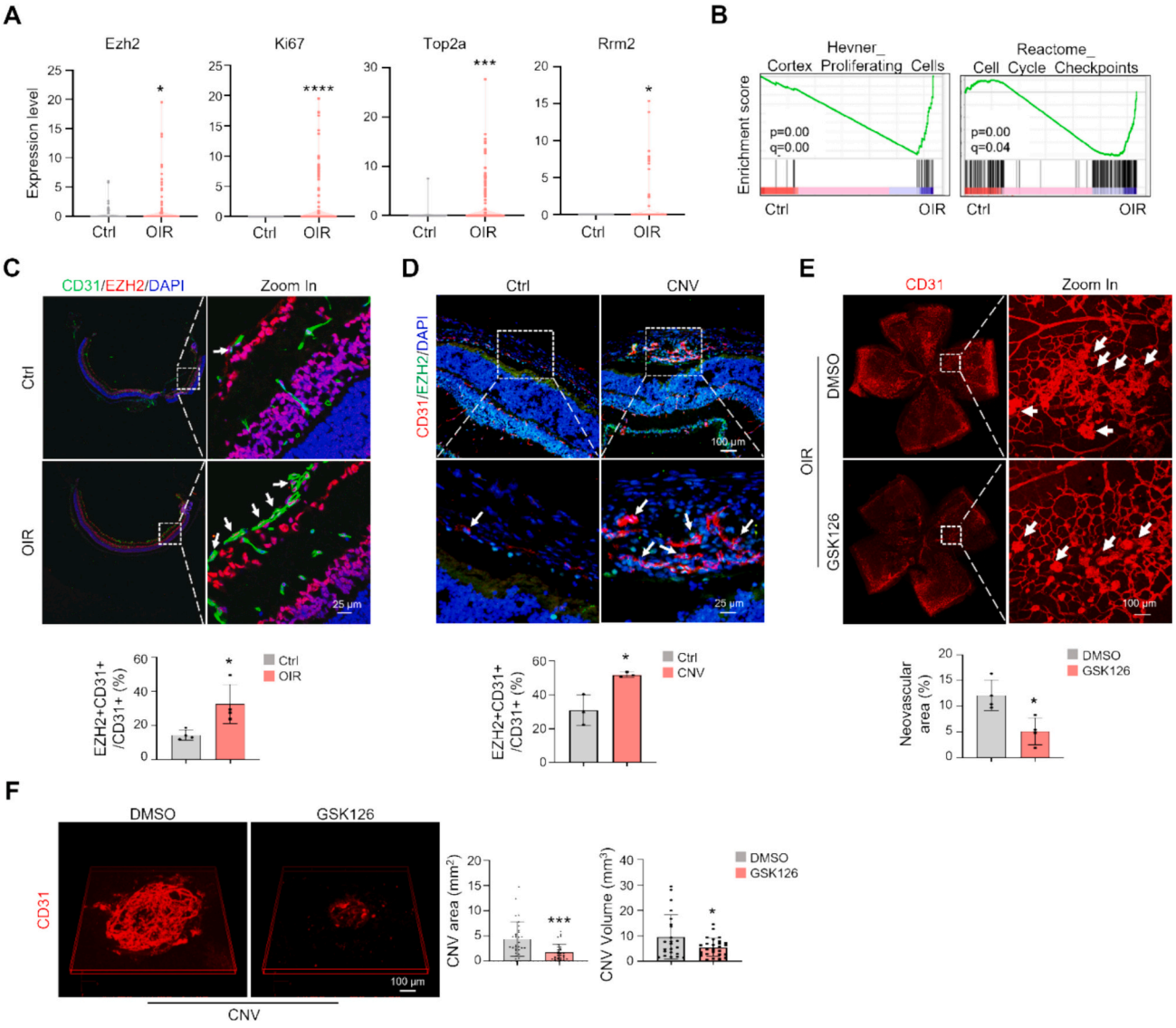

Fig. 6. Pharmacological inhibition of EZH2 suppresses pathological ocular angiogenesis. A Comparative analysis of Ezh2 and proliferation markers (Ki67, Top2a, Rrm2) expression levels between OIR and control groups in the published scRNA-seq dataset (PRJNA864092). B GSEA of proliferation- and cell cycle-related genes from published scRNA- seq data shown in (A). C Immunofluorescence confocal microscopy of retinal cross-sections from OIR (P17) and control mice stained with anti-CD31, anti-EZH2, demonstrating EZH2 co-localization with $CD31^+$ ECs (n = 4). The white arrows indicate $EZH2^+$ ECs. D Immunofluorescence confocal microscopy of choroidal cross-sections from CNV d7 and control mice stained with anti-CD31, anti-EZH2, demonstrating EZH2 co-localization with $CD31^+$ ECs (n = 3). The white arrows indicate $EZH2^+$ ECs. E Quantitative analysis of pathological neovascularization in flat-mounted retinas from P17 OIR mice treated with GSK126 or DMSO (n = 4). The white arrows indicate the neovascularization area. F Whole choroidal tissues were flat mounted and stained with CD31 antibody at d7. Confocal images were taken. The CNV area and volumes were compared between GSK126 and DMSO injected mice ($n = 26$ laser spots for Ctrl; $n = 31$ laser spots for GSK126). Bars = means ± SD. *, $p < 0.05$; ***, $p < 0.001$; ****, $p < 0.0001$. Statistical tests: two-tailed Student's *t*-test for A, C-F.

and angiogenesis appears highly context-dependent. For instance, while Mitić et al. reported that EZH2 modulation improved neovascularization and functional recovery in a murine hindlimb ischemia model [57], Tsou et al. found that EZH2 inhibition preserved normal angiogenesis in scleroderma [50]. These apparently contradictory findings highlight that the net effects of EZH2 on angiogenesis may be determined by tissue-specific microenvironments or pathological conditions. The precise molecular mechanisms underlying these differential responses remain to be fully elucidated and require further investigations.

Previous work by the Benedito group revealed that Notch signaling exerts temporally and context-dependent regulation of EC proliferation during sprouting angiogenesis [54]. Their studies showed that Notch inhibition at the angiogenic front – where proliferation is most active – leads to enhanced ERK signaling, resulting in upregulation of the cell cycle inhibitor p21 and subsequent suppression of EC proliferation. Conversely, in quiescent and mature ECs, Notch blockade produces a more modest elevation of ERK activity that paradoxically stimulates proliferation [54,58]. Although our current study has characterized the overall vascular phenotypes in vivo, the precise regulation of EC proliferation dynamics by the Notch-EZH2 axis under physiological conditions remains to be elucidated. Future investigations employing advanced single-cell resolution techniques, particularly mosaic analysis with lineage tracing [7,58], will be essential to dissect the spatiotemporal control of EC proliferation by the Notch-EZH2 axis in vivo.

Notch signaling has been well-documented as a critical regulator governing both tip/stalk cell fate decisions and arterial-venous specification during angiogenesis [7,8,11,12]. Our results demonstrated that EZH2 knockdown fails to significantly alter the expression of tip/stalk cell markers or arteriovenous differentiation markers. Moreover, ectopic EZH2 expression showed no observable impact on Notch-mediated

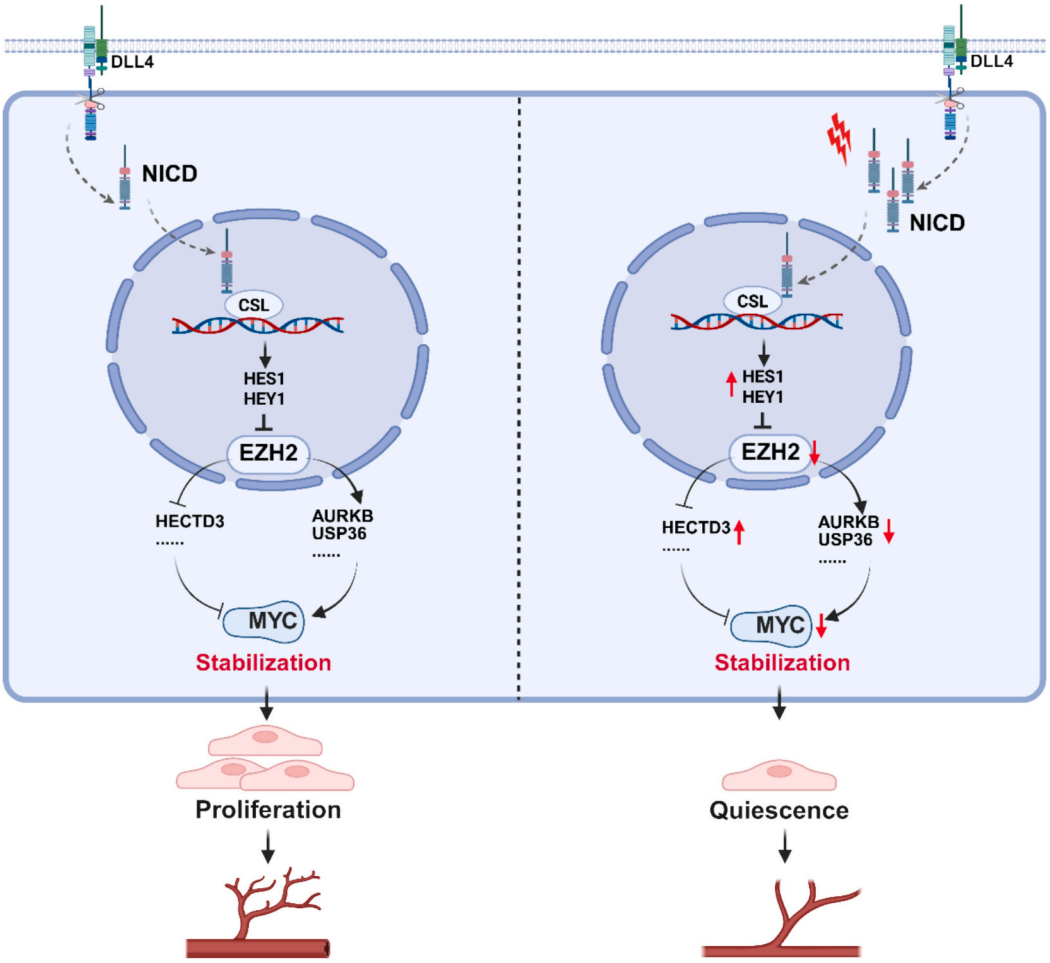

Fig. 7. Schematic diagram. Under physiological conditions (left), EZH2, under negative regulation by Notch signal, maintains MYC protein homeostasis through upregulating stabilization factors and downregulating destabilization factors, thereby promoting EC proliferation and angiogenesis. Upon enhanced Notch signal activity (right), transcription factors such as HES1 and HEY1 transcriptionally suppresses EZH2 expression. This leads to MYC protein destabilization by reducing stabilization factors while enhancing destabilization factors, ultimately inducing EC quiescence and suppressing angiogenesis.

regulation, suggesting that EZH2 operates independently of the Notch signaling in regulating these EC differentiation programs. While our in vitro data clearly demonstrate this functional dissociation, the potential in vivo role of EZH2 in modulating these processes requires more comprehensive genetic investigations in the future [7,12].

Emerging evidence suggests that EZH2 coordinates multiple downstream mechanisms to regulate endothelial homeostasis, angiogenesis, and inflammation, including canonical PRC2-dependent gene silencing, non-canonical transcriptional regulation, and metabolic reprogramming [15]. Previous studies by our group and others have established that the transcription factor MYC, directly or indirectly repressed by Notch signal, serves as a master regulator of EC proliferation in both physiological and pathological angiogenesis [7,10,11,13]. MYC could exert its effects through diverse molecular mechanisms that modulate gene expression, metabolic reprogramming, and cell cycle progression [34]. In the present study, we demonstrate that Notch-dependent downregulation of EZH2 reduces MYC protein abundance and its transcription activity on regulating the expression of cell cycle progression-related and nucleotide synthesis-related genes, resulting consequent impairment of EC proliferative and angiogenic capacities. Notably, MYC overexpression effectively rescued the compromised EC proliferation and sprouting angiogenesis induced by EZH2 inhibition.

MYC is controlled through multilayered regulation, encompassing transcriptional, translational, and post-translational mechanisms [33]. Although prior studies have shown that EZH2 can either directly interact with MYC or indirectly silencing the tumor-suppressor gene SMAD4 to upregulate MYC expression in cancer [23,24], we found that in ECs, EZH2 does not significantly affect MYC transcription and mRNA stability. Instead, EZH2 inhibition promoted phosphorylation of MYC at threonine-58 (T58), leading to protein destabilization. This effect appears independent of miR-218-5p and miR-342-5p, which we previously reported to destabilize MYC by downregulating EYA3 expression [10,11]. Our findings revealed that pharmacological inhibition of EZH2's methyltransferase activity (via GSK126) is sufficient to markedly reduce MYC protein abundance, implying that EZH2 exerts transcriptional control over factors governing MYC stability. Integrative omics profiling coupled experimental validation further demonstrated that EZH2 inhibition downregulated multiple genes involved in MYC protein stabilization while upregulating several MYC-destabilizing factors and downregulating multiple MYC-stabilizing factors [37,38,40,59,60]. Notably, AURKB, a kinase known to phosphorylate and stabilize MYC, was downregulated at both mRNA and protein levels upon EZH2 inhibition, consistent with prior findings by Li et al. [61]. However, whether AURKB mediates the effects of EZH2 on protein stability, as well as the precise mechanisms underlying EZH2-dependent regulation of MYC stability, requires further investigations. In addition, our results revealed that the expression levels of USP36 and HECTD3, two key molecules regulating MYC protein stability, also underwent significant alterations upon EZH2 knockdown. Specifically, USP36 expression was markedly upregulated, while HECTD3 expression was substantially

downregulated. Previous studies have shown that USP36 inhibits MYC degradation by interacting with FBW7, whereas HECTD3 promotes MYC polyubiquitination and subsequent degradation [38,39]. It remains an open question whether EZH2 modulates MYC stability by regulating USP36 and HECTD3.

Aberrant angiogenesis, the uncontrolled formation of new blood vessels, plays a critical role in multiple diseases, including ocular disorders and cancer. The inhibition of EZH2 has emerged as a promising therapeutic strategy for pathological vascular diseases [62], including atherosclerosis [63], pulmonary arterial hypertension (PAH) [64], and tumor progression [65]. In ocular contexts, Wan et al. previously established that EZH2 inhibition attenuates angiogenesis in a corneal neovascularization model [20]. Our current study extends these findings by demonstrating a marked upregulation of EZH2 expression in ECs during the progression of OIR and CNV. Notably, pharmacological intervention with the EZH2 inhibitor GSK126 significantly suppressed pathological ocular angiogenesis, providing compelling evidence that EZH2 represents a viable therapeutic target for hyper-angiogenesis-related ocular diseases. In addition, previous studies indicated that EZH2 modulates angiogenesis through transcriptional regulation of VEGF signaling pathway [18,19]. Given that anti-VEGF agents represent the cornerstone of current therapeutic strategies for intraocular neovascular disorders [5], investigating potential synergistic effects between EZH2 inhibition and conventional anti-VEGF therapy might be a compelling avenue for translational research. In addition, our findings demonstrate that pharmacological inhibition of MYC can also effectively suppress pathological neovascularization in the OIR model. However, given the broad physiological roles of MYC, its systemic inhibition may lead to unintended off-target effects [66]. Therefore, further comprehensive evaluation is warranted to determine its suitability as a therapeutic target for intraocular neovascular disorder.

In summary, our study has unveiled a tripartite regulatory network wherein Notch negatively regulates EZH2 to control MYC-dependent EC proliferation and angiogenesis. The translational significance is highlighted by EZH2 inhibitor's efficacy in ocular neovascularization models, proposing EZH2 as a therapeutic target for diseases like ROP and AMD.

CRediT authorship contribution statement

Yanyan Duan: Project administration, Investigation, Formal analysis. **Ting Wen:** Validation, Investigation, Data curation. **Jingli Ma:** Validation, Formal analysis. **Yuxin Chen:** Methodology, Investigation. **Liang Liang:** Validation. **Ziyan Yang:** Funding acquisition, Data curation. **Peiran Zhang:** Validation, Funding acquisition. **Quan Zhang:** Investigation. **Manhong Li:** Methodology. **Xingxing Feng:** Validation. **Danni Jia:** Validation. **Shanqiang Luo:** Validation. **Jiaxing Sun:** Writing – review & editing, Writing – original draft, Supervision, Funding acquisition. **Hua Han:** Writing – review & editing, Supervision, Funding acquisition, Conceptualization. **Xianchun Yan:** Writing – review & editing, Writing – original draft, Supervision, Funding acquisition, Conceptualization.

Declaration of competing interest

The authors declare no conflict of interest.

Acknowledgements

This work was supported by the National Natural Science Foundation (32270966, 82370403, 82303370, 82403385) of China, Natural Science Foundation of Shaanxi Province (2024JC-YBMS-667), Open competition mechanism to select the best candidate for key research projects of Ningxia Medical University (XJKF240308, XJKF240309).

Appendix A. Supplementary data

Supplementary data to this article can be found online at https://doi.org/10.1016/j.lfs.2025.123889.

Data availability

Data will be made available on request.

References

[1] A.C. Dudley, A.W. Griffioen, Pathological angiogenesis: mechanisms and therapeutic strategies, Angiogenesis 26 (3) (2023) 313–347.
[2] G. Eelen, L. Treps, X. Li, P. Carmeliet, Basic and therapeutic aspects of angiogenesis updated, Circ. Res. 127 (2) (2020) 310–329.
[3] Z.L. Liu, H.H. Chen, L.L. Zheng, L.P. Sun, L. Shi, Angiogenic signaling pathways and anti-angiogenic therapy for cancer, Signal Transduct. Target. Ther. 8 (1) (2023) 198.
[4] Q. Zhang, X. Yan, H. Han, Y. Wang, J. Sun, Pericyte in retinal vascular diseases: a multifunctional regulator and potential therapeutic target, FASEB J. 38 (10) (2024) e23679.
[5] Y. Cao, R. Langer, N. Ferrara, Targeting angiogenesis in oncology, ophthalmology and beyond, Nat. Rev. Drug Discov. 22 (6) (2023) 476–495.
[6] A. Akil, A.K. Gutierrez-Garcia, R. Guenter, J.B. Rose, A.W. Beck, H. Chen, et al., Notch signaling in vascular endothelial cells, angiogenesis, and tumor progression: an update and prospective, Front. Cell Dev. Biol. 9 (2021) 642352.
[7] W. Luo, I. Garcia-Gonzalez, M. Fernandez-Chacon, V. Casquero-Garcia, M. S. Sanchez-Munoz, S. Muhleder, et al., Arterialization requires the timely suppression of cell growth, Nature 589 (7842) (2021) 437–441.
[8] L.A. Naiche, S.R. Villa, J.K. Kitajewski, Endothelial cell fate determination: a top Notch job in vascular decision-making, Cold Spring Harb. Perspect. Med. 12 (11) (2022) a041183.
[9] C. Marziano, G. Genet, K.K. Hirschi, Vascular endothelial cell specification in health and disease, Angiogenesis 24 (2) (2021) 213–236.
[10] J.X. Sun, G.R. Dou, Z.Y. Yang, L. Liang, J.L. Duan, B. Ruan, et al., Notch activation promotes endothelial quiescence by repressing MYC expression via miR-218, Mol. Ther. Nucleic Acids. 25 (2021) 554–566.
[11] X. Zhang, J. Sun, P. Zhang, T. Wen, R. Wang, L. Liang, et al., miR-342-5p downstream to Notch enhances arterialization of endothelial cells in response to shear stress by repressing MYC, Mol. Ther. Nucleic Acids. 32 (2023) 343–358.
[12] M. Fernandez-Chacon, S. Muhleder, A. Regano, L. Garcia-Ortega, S.F. Rocha, C. Torroja, et al., Incongruence between transcriptional and vascular pathophysiological cell states, Nat. Cardiovasc. Res. 2 (2023) 2023530–2023549.
[13] J. Masek, E.R. Andersson, Jagged-mediated development and disease: mechanistic insights and therapeutic implications for Alagille syndrome, Curr. Opin. Cell Biol. 86 (2024) 102302.
[14] X. Yan, Z. Yang, X. Cao, L. Liang, Y. Duan, P. Zhang, et al., Targeting endothelial MYC using siRNA or miR-218 nanoparticles sensitizes chemo- and immunotherapies by recapitulating the Notch activation-induced tumor vessel normalization, Theranostics 15 (11) (2025) 5381–5401.
[15] L. Sun, X. Li, H. Luo, H. Guo, J. Zhang, Z. Chen, et al., EZH2 can be used as a therapeutic agent for inhibiting endothelial dysfunction, Biochem. Pharmacol. 213 (2023) 115594.
[16] M. Maleszewska, B. Vanchin, M.C. Harmsen, G. Krenning, The decrease in histone methyltransferase EZH2 in response to fluid shear stress alters endothelial gene expression and promotes quiescence, Angiogenesis 19 (1) (2016) 9–24.
[17] P. Zhang, X. Yan, X. Zhang, Y. Liu, X. Feng, Z. Yang, et al., TMEM215 prevents endothelial cell apoptosis in vessel regression by blunting BIK-regulated ER-to-mitochondrial ca influx, Circ. Res. 133 (9) (2023) 739–757.
[18] Y. Shi, J. Li, H. Chen, Y. Hu, L. Tang, Y. Wang, et al., Inhibition of EZH2 suppresses peritoneal angiogenesis by targeting a VEGFR2/ERK1/2/HIF-1alpha-dependent signaling pathway, J. Pathol. 258 (2) (2022) 164–178.
[19] Y.T. Chen, F. Zhu, W.R. Lin, R.B. Ying, Y.P. Yang, L.H. Zeng, The novel EZH2 inhibitor, GSK126, suppresses cell migration and angiogenesis via down-regulating VEGF-A, Cancer Chemother. Pharmacol. 77 (4) (2016) 757–765.
[20] S.S. Wan, Y.M. Pan, W.J. Yang, Z.Q. Rao, Y.N. Yang, Inhibition of EZH2 alleviates angiogenesis in a model of corneal neovascularization by blocking FoxO3a-mediated oxidative stress, FASEB J. 34 (8) (2020) 10168–10181.
[21] K. Pappas, T.C. Martin, A.L. Wolfe, C.B. Nguyen, T. Su, J. Jin, et al., NOTCH and EZH2 collaborate to repress PTEN expression in breast cancer, Commun. Biol. 4 (1) (2021) 312.
[22] M. Bottcher, H. Bruns, S. Volkl, J. Lu, E. Chartomatsidou, N. Papakonstantinou, et al., Control of PD-L1 expression in CLL-cells by stromal triggering of the Notch-c-Myc-EZH2 oncogenic signaling axis, J. Immunother. Cancer 9 (4) (2021) e001889.
[23] Q. Zhang, Y. Shi, S. Liu, W. Yang, H. Chen, N. Guo, et al., EZH2/G9a interact to mediate drug resistance in non-small-cell lung cancer by regulating the SMAD4/ERK/c-Myc signaling axis, Cell Rep. 43 (2) (2024) 113714.
[24] L. Wang, C. Chen, Z. Song, H. Wang, M. Ye, D. Wang, et al., EZH2 depletion potentiates MYC degradation inhibiting neuroblastoma and small cell carcinoma tumor formation, Nat. Commun. 13 (1) (2022) 12.
[25] X.C. Yan, J. Cao, L. Liang, L. Wang, F. Gao, Z.Y. Yang, et al., miR-342-5p is a Notch downstream molecule and regulates multiple angiogenic pathways including

Notch, vascular endothelial growth factor and transforming growth factor beta signaling, J. Am. Heart Assoc. 5 (2) (2016) e003042.
[26] P. Zhang, K. Yue, X. Liu, X. Yan, Z. Yang, J. Duan, et al., Endothelial Notch activation promotes neutrophil transmigration via downregulating endomucin to aggravate hepatic ischemia/reperfusion injury, Sci. China Life Sci. 63 (3) (2020) 375–387.
[27] X. Zhang, X. Yan, J. Cao, Z. Yang, X. Cao, Y. Zhang, et al., SM22α^{+} vascular mural cells are essential for vessel stability in tumors and undergo phenotype transition regulated by Notch signaling, J. Exp. Clin. Cancer Res. 39 (1) (2020) 124.
[28] J.X. Sun, T.F. Chang, M.H. Li, L.J. Sun, X.C. Yan, Z.Y. Yang, et al., SNAI1, an endothelial-mesenchymal transition transcription factor, promotes the early phase of ocular neovascularization, Angiogenesis 21 (3) (2018) 635–652.
[29] S.S. Hasan, A. Fischer, Notch signaling in the vasculature: angiogenesis and angiocrine functions, Cold Spring Harb. Perspect. Med. 13 (2) (2023) a041166.
[30] A. Fischer, M. Gessler, Delta-Notch–and then? Protein interactions and proposed modes of repression by Hes and Hey bHLH factors, Nucleic Acids Res. 35 (14) (2007) 4583–4596.
[31] G.R. Dou, L. Wang, Y.S. Wang, H. Han, Notch signaling in ocular vasculature development and diseases, Mol. Med. 18 (1) (2012) 47–55.
[32] W. Chen, P. Xia, H. Wang, J. Tu, X. Liang, X. Zhang, et al., The endothelial tip-stalk cell selection and shuffling during angiogenesis, J. Cell Commun. Signal. 13 (3) (2019) 291–301.
[33] M. Kalkat, J. De Melo, K.A. Hickman, C. Lourenco, C. Redel, D. Resetca, et al., MYC deregulation in primary human cancers, Genes (Basel) 8 (6) (2017) 151.
[34] S.K. Das, B.A. Lewis, D. Levens, MYC: a complex problem, Trends Cell Biol. 33 (3) (2023) 235–246.
[35] P. Hydbring, A. Castell, L.G. Larsson, MYC modulation around the CDK2/p27/SKP2 Axis, Genes (Basel) 8 (7) (2017) 174.
[36] L. Zhang, H. Zhou, X. Li, R.L. Vartuli, M. Rowse, Y. Xing, et al., Eya3 partners with PP2A to induce c-Myc stabilization and tumor progression, Nat. Commun. 9 (1) (2018) 1047.
[37] J. Jiang, J. Wang, M. Yue, X. Cai, T. Wang, C. Wu, et al., Direct phosphorylation and stabilization of MYC by aurora B kinase promote T-cell leukemogenesis, Cancer Cell 37 (2) (2020), 200–15.e5.
[38] G. Zhang, Q. Zhu, X. Yan, M. Ci, E. Zhao, J. Hou, et al., HECTD3 promotes gastric cancer progression by mediating the polyubiquitination of c-MYC, Cell Death Dis. 8 (1) (2022) 185.
[39] X.X. Sun, X. He, L. Yin, M. Komada, R.C. Sears, M.S. Dai, The nucleolar ubiquitin-specific protease USP36 deubiquitinates and stabilizes c-Myc, Proc. Natl. Acad. Sci. USA 112 (12) (2015) 3734–3739.
[40] Z. Wang, H. Cai, Z. Li, W. Sun, E. Zhao, H. Cui, Histone demethylase KDM4B accelerates the progression of glioblastoma via the epigenetic regulation of MYC stability, Clin. Epigenetics 15 (1) (2023) 192.
[41] Z.Y. Zhou, T.F. Chang, Z.B. Lin, Y.T. Jing, L.S. Wen, Y.L. Niu, et al., Microglial Galectin3 enhances endothelial metabolism and promotes pathological angiogenesis via Notch inhibition by competitively binding to Jag1, Cell Death Dis. 14 (6) (2023) 380.
[42] R. Ren, S. Ding, K. Ma, Y. Jiang, Y. Wang, J. Chen, et al., SUMOylation fine-tunes endothelial HEY1 in the regulation of angiogenesis, Circ. Res. 134 (2) (2024) 203–222.
[43] X.X. Yao, J.B. Lu, Z.D. Ye, L. Zheng, Q. Wang, Z.Q. Lin, et al., Hairy/enhancer of split homologue-1 suppresses vascular endothelial growth factor-induced angiogenesis via downregulation of osteopontin expression, Sci. Rep. 7 (1) (2017) 898.
[44] C. Wiese, J. Heisig, M. Gessler, Hey bHLH factors in cardiovascular development, Pediatr. Cardiol. 31 (3) (2010) 363–370.
[45] C. Lu, H.D. Han, L.S. Mangala, R. Ali-Fehmi, C.S. Newton, L. Ozbun, et al., Regulation of tumor angiogenesis by EZH2, Cancer Cell 18 (2) (2010) 185–197.
[46] E. Riquelme, M. Suraokar, C. Behrens, H.Y. Lin, L. Girard, M.B. Nilsson, et al., VEGF/VEGFR-2 upregulates EZH2 expression in lung adenocarcinoma cells and EZH2 depletion enhances the response to platinum-based and VEGFR-2-targeted therapy, Clin. Cancer Res. 20 (14) (2014) 3849–3861.
[47] M. Smits, S.E. Mir, R.J. Nilsson, P.M. van der Stoop, J.M. Niers, V.E. Marquez, et al., Down-regulation of miR-101 in endothelial cells promotes blood vessel formation through reduced repression of EZH2, PLoS One 6 (1) (2011) e16282.
[48] M. Maleszewska, R.A. Gjaltema, G. Krenning, M.C. Harmsen, Enhancer of zeste homolog-2 (EZH2) methyltransferase regulates transgelin/smooth muscle-22alpha expression in endothelial cells in response to interleukin-1beta and transforming growth factor-beta2, Cell. Signal. 27 (8) (2015) 1589–1596.
[49] J.S. Fang, B.G. Coon, N. Gillis, Z. Chen, J. Qiu, T.W. Chittenden, et al., Shear-induced Notch-Cx37-p27 axis arrests endothelial cell cycle to enable arterial specification, Nat. Commun. 8 (1) (2017) 2149.
[50] P.S. Tsou, P. Campbell, M.A. Amin, P. Coit, S. Miller, D.A. Fox, et al., Inhibition of EZH2 prevents fibrosis and restores normal angiogenesis in scleroderma, Proc. Natl. Acad. Sci. USA 116 (9) (2019) 3695–3702.
[51] K. Bentley, S. Chakravartula, The temporal basis of angiogenesis, Philos. Trans. R. Soc. Lond. Ser. B Biol. Sci. 372 (1720) (2017) 20150522.
[52] H.W. Jeong, B. Hernandez-Rodriguez, J. Kim, K.P. Kim, R. Enriquez-Gasca, J. Yoon, et al., Transcriptional regulation of endothelial cell behavior during sprouting angiogenesis, Nat. Commun. 8 (1) (2017) 726.
[53] F. Chen, Z. Deng, X. Wang, Y. Liu, K. Zhao, Y. Zhang, et al., DDX24 spatiotemporally orchestrates VEGF and Wnt signaling during developmental angiogenesis, Proc. Natl. Acad. Sci. USA 122 (19) (2025) e2417445122.
[54] S. Muhleder, M. Fernandez-Chacon, I. Garcia-Gonzalez, R. Benedito, Endothelial sprouting, proliferation, or senescence: tipping the balance from physiology to pathology, Cell. Mol. Life Sci. 78 (4) (2021) 1329–1354.
[55] K. Wilhelm, K. Happel, G. Eelen, S. Schoors, M.F. Oellerich, R. Lim, et al., FOXO1 couples metabolic activity and growth state in the vascular endothelium, Nature 529 (7585) (2016) 216–220.
[56] J. Andrade, C. Shi, A.S.H. Costa, J. Choi, J. Kim, A. Doddaballapur, et al., Control of endothelial quiescence by FOXO-regulated metabolites, Nat. Cell Biol. 23 (4) (2021) 413–423.
[57] T. Mitic, A. Caporali, I. Floris, M. Meloni, M. Marchetti, R. Urrutia, et al., EZH2 modulates angiogenesis in vitro and in a mouse model of limb ischemia, Mol. Ther. 23 (1) (2015) 32–42.
[58] S. Pontes-Quero, M. Fernandez-Chacon, W. Luo, F.F. Lunella, V. Casquero-Garcia, I. Garcia-Gonzalez, et al., High mitogenic stimulation arrests angiogenesis, Nat. Commun. 10 (1) (2019) 2016.
[59] Z. Mei, D. Zhang, B. Hu, J. Wang, X. Shen, W. Xiao, FBXO32 targets c-Myc for proteasomal degradation and inhibits c-Myc activity, J. Biol. Chem. 290 (26) (2015) 16202–16214.
[60] S.Y. Kim, A. Herbst, K.A. Tworkowski, S.E. Salghetti, W.P. Tansey, Skp2 regulates Myc protein stability and activity, Mol. Cell 11 (5) (2003) 1177–1188.
[61] M. Li, D. Liu, F. Xue, H. Zhang, Q. Yang, L. Sun, et al., Stage-specific dual function: EZH2 regulates human erythropoiesis by eliciting histone and non-histone methylation, Haematologica 108 (9) (2023) 2487–2502.
[62] J.L. Yuan, C.Y. Yin, Y.Z. Li, S. Song, G.J. Fang, Q.S. Wang, EZH2 as an epigenetic regulator of cardiovascular development and diseases, J. Cardiovasc. Pharmacol. 78 (2) (2021) 192–201.
[63] X. Wei, Y. Zhang, L. Xie, K. Wang, X. Wang, Pharmacological inhibition of EZH2 by GSK126 decreases atherosclerosis by modulating foam cell formation and monocyte adhesion in apolipoprotein E-deficient mice, Exp. Ther. Med. 22 (2) (2021) 841.
[64] Z.L. Shi, K. Fang, Z.H. Li, D.H. Ren, J.Y. Zhang, J. Sun, EZH2 inhibition ameliorates transverse aortic constriction-induced pulmonary arterial hypertension in mice, Can. Respir. J. 2018 (2018) 9174926.
[65] C. Qian, C. Yang, Y. Tang, W. Zheng, Y. Zhou, S. Zhang, et al., Pharmacological manipulation of Ezh2 with salvianolic acid B results in tumor vascular normalization and synergizes with cisplatin and T cell-mediated immunotherapy, Pharmacol. Res. 182 (2022) 106333.
[66] P.E. Thompson, J. Shortt, Defeating MYC with drug combinations or dual-targeting drugs, Trends Pharmacol. Sci. 45 (6) (2024) 490–502.